Microbial Cell Factories

RESEARCH Open Access

Region-based segmental swapping of homologous enzymes for higher cadaverine production

Seungjin Kim[1,2†], Dae-yeol Ye[1†], Hyun Gyu Lim[2], Myung Hyun Noh[3*], Jae-Seong Yang[4*] and Gyoo Yeol Jung[1,5*]

Abstract

Background Cadaverine, displaying potential in medicine, agriculture and polyamide production, is biologically produced through L-lysine decarboxylation. Considering the potential of the polyamide market, its biological production has been focused on with following diverse efforts to improve the production. In *Escherichia coli*, lysine decarboxylase exists in two forms: CadA and LdcC, and it is known that CadA exhibits superior catalytic activity compared to LdcC. Despite its potential, cadaverine production is limited due to increased intracellular pH, which destabilizes the decameric structure of CadA and inhibits its activity.

Results In this study, based on the structural analysis, a chimeric CadA enzyme, CL2, was engineered by replacing its pH-sensitive region with a structurally stable counterpart derived from LdcC. The resulting BLCL2 strain with CL2 produced 1.12 g/L of cadaverine—1.96 times higher than BLC strain with the wild type CadA in flask culture. Compared to the wild type CadA, structural modifications enhanced pH stability and improved the affinity of CadA toward pyridoxal 5-phosphate (PLP), its cofactor.

Conclusions This study developed the improved strains for cadaverine production by creating the new enzyme, which is validated by enhanced amount of cadaverine. In addition, the segmental swapping guided by structure analysis was exhibited as the one of effective method in protein engineering strategies. These advancements offer a promising approach to optimizing cadaverine biosynthesis for industrial applications.

Keywords Cadaverine, Chimeric enzyme, Lysine decarboxylase, pH stability, Cofactor affinity

†Seungjin Kim and Dae-yeol Ye contributed equally to this work.

*Correspondence:
Myung Hyun Noh
mhnoh@krict.re.kr
Jae-Seong Yang
jaeseong.yang@cragenomica.es
Gyoo Yeol Jung
gyjung@postech.ac.kr
[1]Department of Chemical Engineering, Pohang University of Science and Technology, 77 Cheongam-Ro, Nam-Gu, Pohang 37673, Gyeongbuk, Korea
[2]Department of Biological Sciences and Bioengineering, Inha University, 100 Inha-Ro, Michuhol-Gu, Incheon 22212, Korea
[3]Research Center for Bio-based Chemistry, Korea Research Institute of Chemical Technology (KRICT), 406-30, Jongga-ro, Jung-gu, Ulsan 44429, Korea
[4]Centre for Research in Agricultural Genomics (CRAG), CSIC-IRTA-UAB-UB, Campus UAB, Bellaterra, Barcelona 08193, Spain
[5]School of Interdisciplinary Bioscience and Bioengineering, Pohang University of Science and Technology, 77 Cheongam-Ro, Nam-Gu, Pohang 37673, Gyeongbuk, Korea

Background

Cadaverine, a C5 diamine molecule, is naturally synthesized in many organisms, where it plays a role in intracellular pH regulation, growth, and defense mechanisms against pathogens; it also has potential applications in medicine and agriculture [1–5]. Cadaverine has gained attention as a monomer of polyamides that serves as an alternative to various diamines produced through petrochemical processes [6–8]. Given its potential in the growing polyamide market, numerous efforts have been made to produce cadaverine from renewable carbon resources or lysine through fermentation or bioconversion, respectively, and industrial strains, including *Escherichia coli* have been used for large-scale production of cadaverine [8–11].

Cadaverine can be biologically produced from L-lysine through decarboxylation catalyzed by lysine decarboxylase with pyridoxal 5-phosphate (PLP) as a cofactor (Fig. 1a) [12, 13]. In *E. coli*, two types of lysine decarboxylases, LdcC and CadA, with different characteristics, have been identified [14, 15]. Although LdcC is constitutively expressed and structurally stable over a broad pH range, it exhibits lower catalytic activity. In contrast, CadA is inducibly expressed in acidic environments and remains stable only at low pH conditions (pH 5.5–6.5), but it shows higher catalytic performance [16, 17]. This regulation of CadA helps the cell maintain an intracellular pH level by scavenging protons through cadaverine biosynthesis only in an acidic condition [15, 18]. Natural enzymes have evolved to support cellular adaptation and survival, and specialized for distinct functions and environmental conditions, each having developed specific advantages compared to other homologous enzymes. However, the low activity of CadA under alkaline conditions, inevitably created during cadaverine synthesis, is known to be a critical limitation for the economic

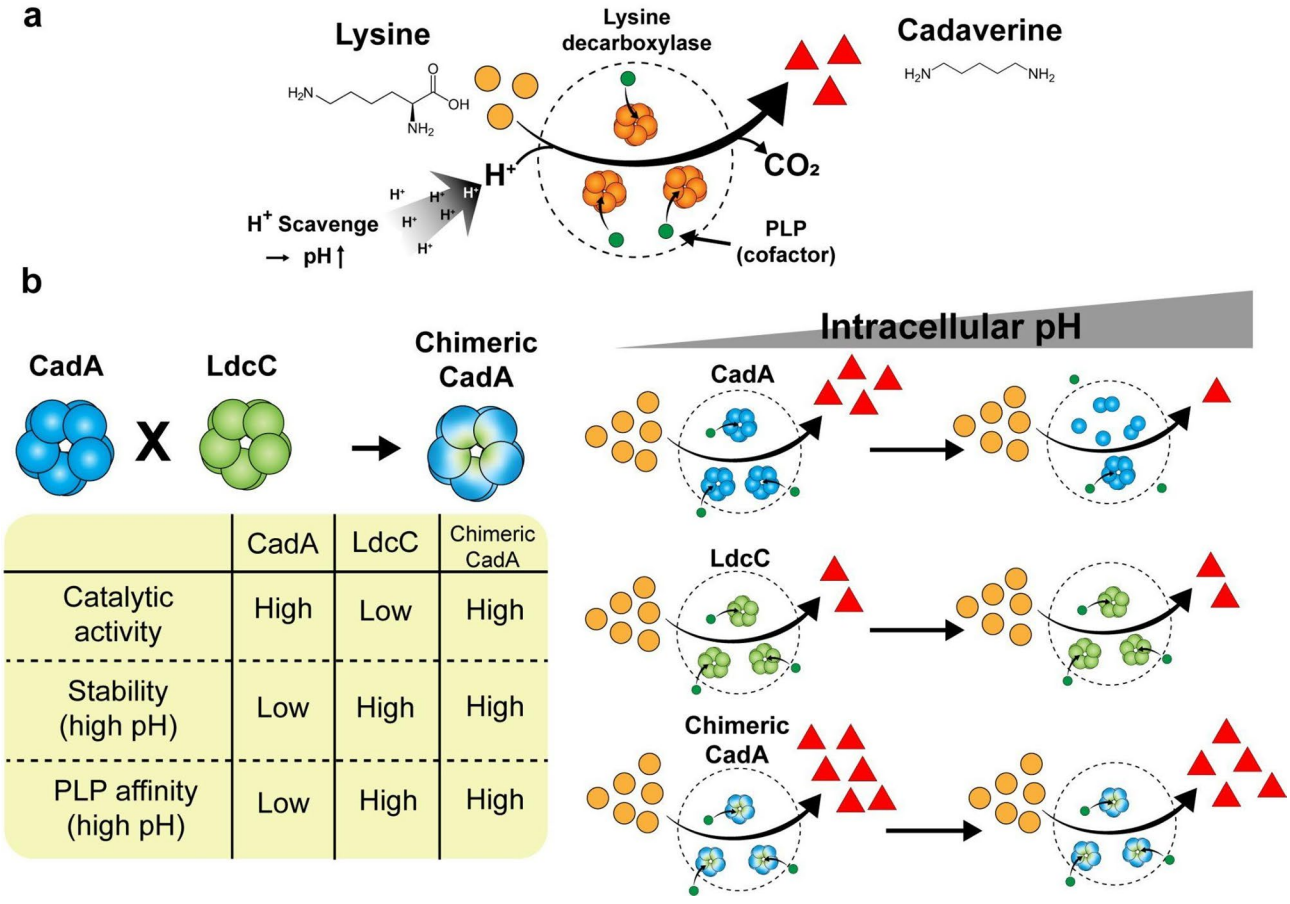

	CadA	LdcC	Chimeric CadA
Catalytic activity	High	Low	High
Stability (high pH)	Low	High	High
PLP affinity (high pH)	Low	High	High

Fig. 1 Overall scheme to improve the cadaverine production in this study
(**A**) Cadaverine synthesis mediated by lysine decarboxylase which catalyzes decarboxylation of lysine leads to the increase of pH level by scavenging protons. Its activity is known to be influenced by the affinity with PLP, the cofactor of lysine decarboxylase. (**B**) There are two different homologous types of lysine decarboxylase in *E. coli*: CadA and LdcC. CadA is known to have higher catalytic activity than LdcC. However, CadA has relatively lower stability of oligomerization on higher pH than LdcC. In this work, two lysine decarboxylases (LdcC and CadA) in *E. coli* were shuffled to create a chimeric mutant with higher enzymatic activity in this study. The chimeric CadA mixed with a partial domain of LdcC showed the enhanced performance in cadaverine conversion from the lysine. Also, the chimeric CadA displayed higher affinity toward the PLP compared to the wild type CadA

production of cadaverine (Fig. 1b) [19]. By combining the specialized advantages of LdcC and CadA, it would be possible to create a novel enzyme for maximizing production in biorefinery applications.

In this study, a chimeric lysine decarboxylase was developed by swapping a partial sequence of LdcC with CadA; this chimeric enzyme showed improved performance in cadaverine production. Structural analysis of LdcC and CadA, which are known to have structural similarities, was conducted, and mutant variants of CadA were created by replacing the partial sequence of CadA with the corresponding sequence of LdcC (Fig. 1b). The effective mutant, CL2, was found to be more stable at high pH and more affinity toward PLP than the wild-type. The mutant strain (BLCL2) with the CL2 mutant could produce 1.12 g/L of cadaverine, which was 1.96-fold higher than that produced by the strain with wild-type CadA (BLC) in flask culture. This chimeric enzyme seems to be helpful in achieving much higher performance in cadaverine production through fermentation or direct conversion from lysine. This study also suggests that creating chimeric enzymes by swapping homologs could overcome the existing limitations exhibited by native enzymes.

Materials and methods

Strains, plasmids, oligonucleotides, and reagents

All bacterial strains and plasmids used in this study are listed in Table S1. All oligonucleotides for plasmid cloning were synthesized by Cosmogenetech (Seoul, Korea) and their sequences are listed in Table S2. The Q5 polymerase for routine PCR was purchased from New England Biolabs (Ipswich, MA, USA). Plasmids were isolated using the Exprep™ Plasmid SV Mini Kit (GeneAll Biotechnology, Seoul, Korea). DNA was purified using the Exprep™ Gel SV kit or the Expin™ CleanUp SV kit (GeneAll Biotechnology, Seoul, Korea). Cell culture reagents, including LB broth and agar, were purchased from BD Biosciences (Sparks, MD, USA). All the reagents were purchased from Sigma-Aldrich (St. Louis, MO, USA).

Plasmid construction

Plasmid pUC_ldcC was constructed using a three-fragment Gibson assembly. The ColE1 origin and kanamycin resistance gene expression cassette were amplified from plasmid pUC_kan using the primers VEC_F and VEC_B. The HCE promoter was synthesized by Thermo Fisher Scientific (Waltham, MA, USA) and amplified using the primers HCE_F and HCE_B. The *ldcC* gene was amplified from *E. coli* genomic DNA using the primers ldcC_genome_F and ldcC_genome_B. The pUC_cadA plasmid was similarly constructed using the primers cadA_genome_F and cadA_genome_B to amplify the *cadA* gene from *E. coli* genomic DNA.

The pUC_CL1 plasmid was constructed with most of its sequence originating from the pUC_cadA plasmid, including the ColE1 origin, kanamycin resistance gene, HCE promoter, and the remaining portion of the *cadA* gene, using CL1_vec_F and CL1_vec_B. Region 1 was specifically amplified from the pUC_ldcC plasmid using primers CL1_ins_F and CL1_ins_B. The two fragments were then assembled using the Gibson assembly. Plasmids pUC_CL2 through pUC_CL6 were constructed in a similar manner, with each respective region (regions 2–6) derived from pUC_ldcC, whereas the rest of the plasmid sequence was sourced from pUC_cadA. The primers CL1_vec_B and CL6_vec_F were identical in sequence to primers HCE_B and VEC_F, respectively. To simplify the experimental process and avoid confusion, identical primers were assigned different names depending on their specific use in plasmid construction.

Cell culture medium and conditions

Cells were cultivated in glucose M9 minimal medium with the following composition: 3 g/L KH_2PO_4, 0.5 g/L NaCl, 6.78 g/L Na_2HPO_4, 1 g/L NH_4Cl, 10 g/L glucose, 0.493 g/L $MgSO_4 \cdot 7\,H_2O$, 0.011 g/L $CaCl_2$. Luria-Bertani (LB) medium containing 5 g/L yeast extract, 10 g/L NaCl, and 10 g/L tryptone was used for plasmid cloning. Kanamycin (50 mg/L) was added for plasmid maintenance. All cell cultures were maintained at 37 °C with agitation at 200 rpm. All cell cultures were performed in triplicate.

For cadaverine production, seed cultures were prepared by inoculating a single colony into 3 mL of LB medium in a 15 mL test tube. After overnight incubation, the seed cultures were diluted in M9 medium at 0.05 OD_{600} an optical density at 600 nm). When the OD_{600} reached between 0.8 and 1.0, the culture was re-diluted into 3 mL of fresh M9 medium contained in a 15 mL test tube or 25 mL of fresh M9 medium contained in 300-mL Erlenmeyer flasks at 0.05 OD_{600} to start the main cultures. In the flask culture, pH was maintained at 7.0, by adding an appropriate amount of 10 M NaOH solution every 6 h.

Enzyme assay

For the cell lysate-based enzyme assay, seed cultures were prepared by inoculating a single colony into 3 mL LB medium. After overnight incubation, the seed cultures were diluted in M9 medium in a 15 mL test tube to 0.05 OD_{600}. When the OD_{600} reached between 0.8 and 1.0, cells were centrifuged to concentrate to an OD_{600} of 4 in a final volume of 1 mL. The cell lysates were prepared using a sonicator (Newtown, CT, USA). For the enzyme activity assay, 10 µL of cell lysate adjusted to contain equal total protein amounts based on Bradford assay was mixed with 90 µL of PBS buffer containing 10 g/L of lysine and various concentrations of PLP.

To estimate the contribution of endogenous PLP from the crude lysate, we performed the following calculation. Cultures were harvested at $OD_{600} = 4$, and the cell pellets were resuspended in 1 mL of PBS prior to sonication. Assuming 8×10^8 cells per mL at $OD_{600} = 1$, the total number of cells in the 1 mL suspension was estimated to be 3.2×10^9. With an average cell volume of 1.16×10^{-12} mL [20], the total cellular volume was calculated to be 3.71×10^{-3} mL. The intracellular concentration of PLP in E. coli has been reported to be approximately 10 µM [21]. Assuming complete release of PLP upon cell lysis, the concentration of endogenous PLP in the lysate was estimated to be 37.1 nM. Since 10 µL of this lysate was used in a 100 µL reaction mixture (1:10 dilution), the final concentration of endogenous PLP in the assay was calculated to be 3.71 nM.

To compare the enzymatic activity in different pH conditions, the activity assays were performed using lysate derived from strains expressing the wild type CadA and CL2, respectively under various initial pH conditions (5, 6, 7, 8, and 9) with 2 mM PLP and 10 g/L lysine. After incubation at 37 °C for 10 min, the reaction was terminated by heating at 90 °C for 20 min. Cadaverine concentrations in the reaction mixtures were analyzed using HPLC.

To determine the enzyme kinetics, enzyme assays were performed using purified enzymes at various lysine concentrations (0.2, 0.4, 1.0 2.0, 4.0, 10.0, and 100.0 mM) under pH 7 with 2 mM PLP. The MagListo His-tagged protein purification kit (Bioneer, Daejeon, Korea) was utilized to purify the 6× His-tagged proteins from cell lysates. Purified enzymes were utilized for assay and concentrations were quantified and adjusted to the same value using the Quick Start Bradford Protein Assay kit (Bio-Rad Laboratories).

Quantification of cell numbers, metabolites

The OD_{600} was measured using a Shimadzu UV-1700 spectrophotometer (Kyoto, Kyoto, Japan). The concentrations of glucose and acetate were analyzed using an ultrafast liquid chromatographic (UFLC) system (Shimadzu LC-20AD) equipped with a Bio-Rad Laboratories Aminex HPX-87H column (Hercules, CA, USA) at 65 °C. H_2SO_4 (5 mM) was used as the mobile phase at a flow rate of 0.6 mL/min. The signals were monitored using a refractive index detector (RID-20 A, Shimadzu). The concentration of cadaverine was determined using a pre-column o-phthalaldehyde derivatization method coupled with reverse-phase liquid column chromatography using Acclaim 120 C18 (3 µm, 4.6 mm x 150 mm, ThermoScientific) [22]. The derivatized cadaverine was eluted at a flow rate of 1.5 mL/min with gradient of acetonitrile, methanol and water (v/v % 45:45:10) solution and 50 mM sodium acetate [23]. The signal was monitored using a UV-Vis diode array detector at a wavelength of 338 nm. The pH was measured using an Orion™ 8103BN ROSS™ pH meter (Thermo Fisher scientific).

Domain analysis and mutant simulation

The number of interacting residues in the dimer and the interaction energy were measured to analyze the contribution of each fragment to the formation of homodimers. Chains A and H from the decameric complex structure of CadA (PDB ID 6YN5) was targeted, which connect to the upper and lower pentameric rings [24]. Then, fragment-specific structures were created and the interacting residues between the two chains that are within a 5 Å distance were identified.

To calculate the free energy of binding for the complex AB, the AnalyseComplex command in FoldX (version 5.0) was used to determine the Gibbs free energies of the complex (ΔG_AB) and of the individual molecules A and B. The interaction energy was calculated using the following formula:

$$\Delta G\_binding = \Delta G\_AB - (\Delta G\_A + \Delta G\_B).$$

Ligand Docking simulation on mutants

Both PLP (PubChem ID: 1051) and lysine (PubChem ID: 5962) were docked into the active site pockets of the CadA, LdcC, and chimeric CadA enzymes (CL1–CL6) using AutoDock Vina within UCSF Chimera software [25]. The protein structures were prepared using EMS-Fold [26], and HDOCK was employed to generate the dimer structures [27]. Prior to docking, hydrogen atoms and charges were added using the default settings. The PLP ligand structure was obtained from the PLP-bound complex structure (PDB ID: 2VYC), whereas the lysine ligand structure was sourced from the RCSB PDB database in CIF format and converted to PDB format using PyMOL software. The ligands were charged before analysis. To refine the docking process, the crystal structure of the PLP-bound arginine decarboxylase (PDB ID: 2VYC) was applied to identify the position of PLP (6 Å) and retained ligands that docked near this site. The target structure of the PLP-bound arginine decarboxylase was aligned to determine the exact location of the PLP-binding site. AutoDock Vina then generated the binding energies (kcal mol^{-1}) for the ligands.

Results

Construction of chimeric variants based on structural analysis of LdcC and CadA

To enhance the overall production of cadaverine, a chimeric CadA mutant was constructed by swapping a certain domain of CadA with corresponding parts derived from LdcC and exploiting their structural and sequence similarities. Although LdcC has lower catalytic activity than CadA, it is known to be more stable at higher pH

[28]. Thus, it was hypothesized that incorporating specific stabilizing domains of LdcC into CadA would prevent subunit dissociation at high pH (Fig. 1). Sequence and structural analysis revealed that CadA and LdcC share 70% sequence similarity and have a high degree of structural similarity (RMSD = 1.58 Å and TM-score 0.98), being allowed to successfully swap the corresponding fragments (Fig. S1). The CadA monomer is composed of five domains: an N-terminal wing domain (residues 1–129), a linker region (residues 130–183), a PLP-binding subdomain (PLP-SD; residues 184–417), subdomain 4 (residues 418–563) and a C-terminal domain (CTD; residues 564–715).

To enable a more precise analysis of the functional role of each subdomain, a subdividing approach was employed instead of domain swapping. Given the structural similarity between these two proteins, it can be inferred that overall structural stability is maintained even in the absence of strict domain swapping. Therefore, the functional domains of CadA were divided into six distinct parts, each consisting of 120 amino acids, and the corresponding fragments of LdcC were substituted with each part to generate chimeric constructs (CL1–CL6; Fig. 2 and Fig. S2).

Validation of the chimeric variants through cadaverine production tests

After the development of chimeric mutants, the activity of the chimeric proteins (CL1 to CL6) was tested, along with that of wild-type LdcC and CadA, by measuring cadaverine production (Fig. 3). Plasmids carrying LdcC, CadA, and each mutant under the control of the HCE promoter, a strong constitutive promoter, were constructed (pUC_LdcC, pUC_CadA, and pUC_CL1–pUC_CL6). These plasmids were introduced into the *E. coli* BL21(DE3) strain, subsequently developing BLL, BLC, and BLCL1 to BLCL6 strains, respectively (Table S1). These strains were cultivated in test tubes containing M9 minimal medium with 10 g/L glucose and cadaverine levels were measured after 24 h of cultivation. Among the variants, the BLCL2 strain carrying CL2 showed cadaverine production 3.0-fold higher than that of the BLC strain, whereas none of the other strains outperformed CL2.

Subsequently, the BLCL2 strain was cultivated along with two control strains (BLL and BLC) in flasks with adjusted pH (Fig. 4). The BLCL2 strain produced a maximum of 1.12 g/L of cadaverine, which is 1.96-fold higher than that of the BLC strain (0.57 g/L), demonstrating the activity of the CL2 mutant is significantly enhanced compared to wild-type CadA. In the cadaverine production of BLCL2 strain, the cadaverine titer slightly decreased at 48 h, likely because of diamine degradation reactions mediated by several transferases (expressed by *speE*, *speG*, and *patA*) [9, 29]. The existence of these reactions could explain the lack of cadaverine production in the BLL strain expressing LdcC under minimal medium conditions. Additional engineering to delete the cadaverine degradation reactions could further enhance cadaverine production. Moreover, compared to the BLL and BLC strains, the BLCL2 strain exhibited growth retardation, likely due to the increased conversion of lysine, an essential component for cell growth, into cadaverine. Additionally, acetate production was reduced in BLCL2, which may be attributed to both the increased redirection of carbon toward cadaverine and the slowed growth rate, leading to decreased production of acetate, a typical byproduct of overflow metabolism that occurs during rapid growth. These data suggest that the CL2 mutant exhibits higher catalytic activity than the wild type and allows for increased production yield during in vivo cultivation.

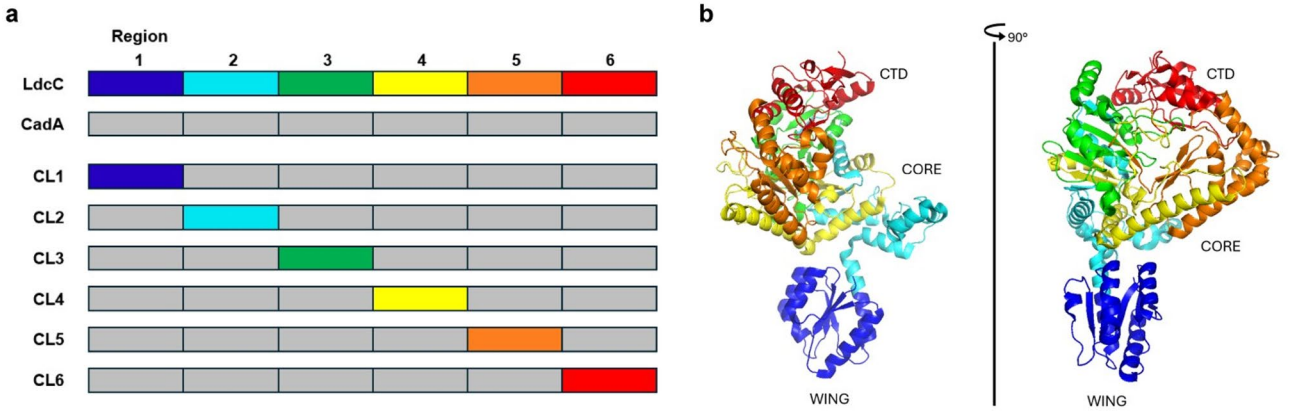

Fig. 2 CadA-based LdcC fragment combinations
(**A**) Schematic representation of the strategy for combining CadA and LdcC to construct six types of mutants (CL1 – CL6). Each mutant was designed using the CadA backbone (gray), with substitutions made for the 1st to 6th fragments of LdcC, shown in blue, cyan, green, yellow, orange, and red, respectively. (**B**) Structure of LdcC highlighting the substituted regions with corresponding colors

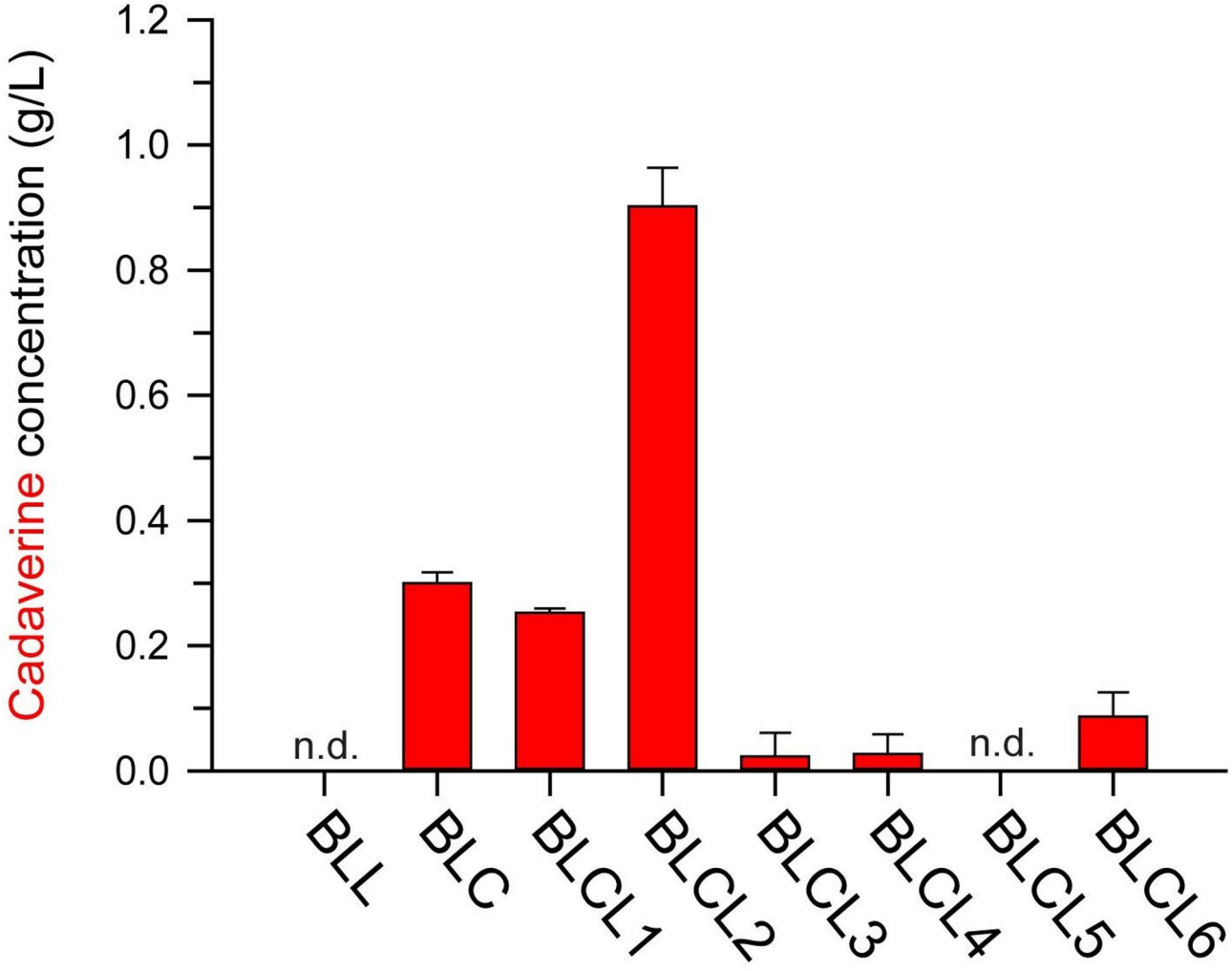

Fig. 3 Validation of constructed mutants in a test-tube scale fermentation
The cadaverine production of BLL, BLC, and BLCL1-6 strains after 24 h cultivation in the test tube. The BLCL2 strain carrying CL2 produced the highest cadaverine concentration indicating that CL2 showed the highest catalytic activity among mutants. The error bars display the standard deviations of three biological replicates ($n = 3$). n.d., not detected

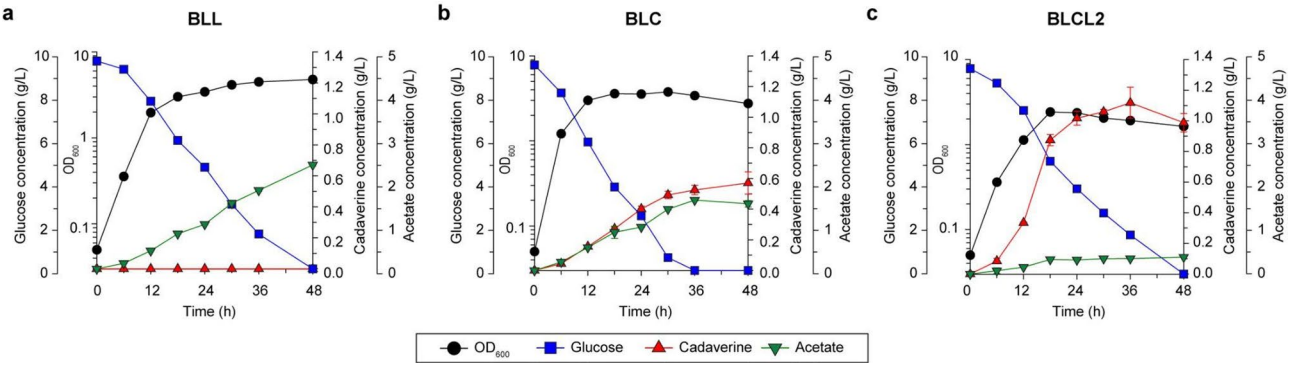

Fig. 4 Fermentation profile of BLL, BLC and BLCL2 strains in flask scale cultivation
Fermentation profiles of (**A**) BLL, (**B**) BLC and (**C**) BLCL2 for 48 h in the modified buffered minimal medium. The x-axis, left y-axis, left offset y-axis, right y-axis, and right y-axis indicate time (h), cell biomass (OD_{600}), glucose concentration (g/L), cadaverine concentration (g/L), and acetate concentration (g/L), respectively. Symbols: black closed circles, OD_{600}; blue closed squares, glucose; red closed triangles, cadaverine; green open inverted triangles, acetate. The error bars indicate the standard deviations of three biological replicates ($n = 3$)

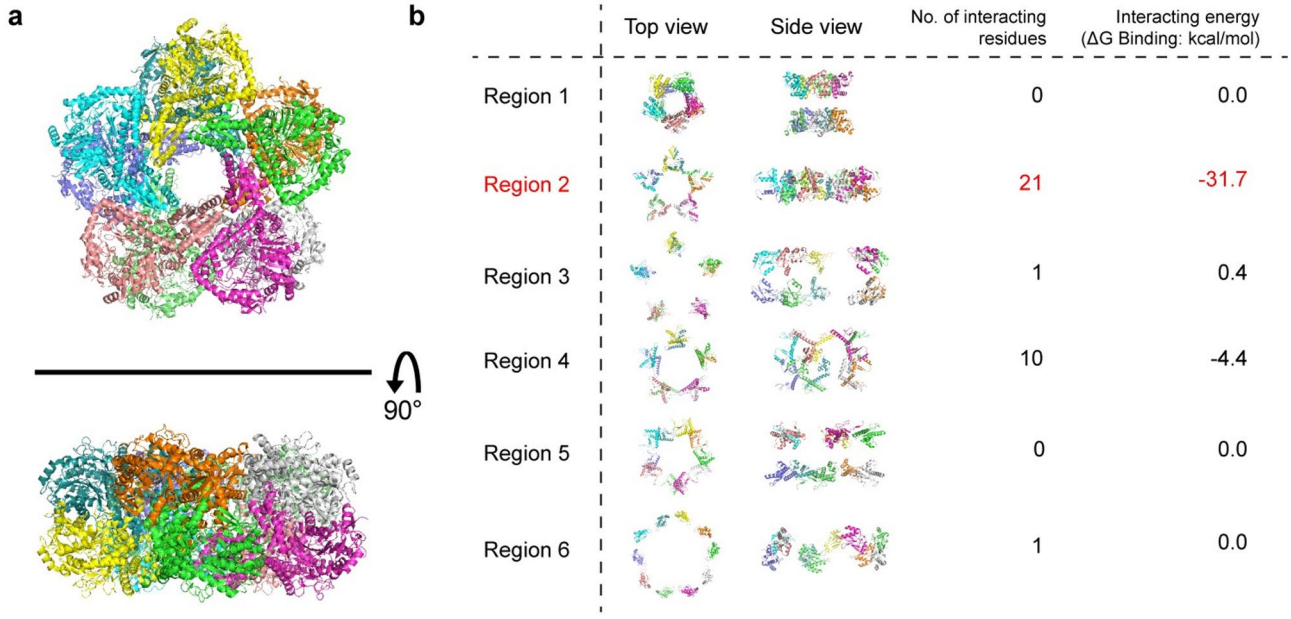

Fig. 5 Analysis of interaction among regions related in the complex formation of CadA decamer
(**A**) The top and side views of CadA decamer complexes. Each chain is colored in a different color. (**B**) Top and side views of the complex, showing only each region individually. The number of residues involved in interactions (< 5 Å) between the subunits of the upper ring and the subunits of the bottom ring within the CadA complex of the decamer has been determined. Interaction energy (ΔG binding) between the region of the dimer

Table 1 AutoDock Vina results for the ligand binding energies (kcal mol^{-1})

Enzyme Name	Ligand	Binding Energy (kcal/mol)
LdcC	Lysine	-4.8
		-4.9
		-4.5
	PLP	-5.7
		-5.9
CadA	Lysine	-4.6
		-4.4
	PLP	-5.3
		-5.4
		-5.5
CL1	-	-
CL2	Lysine	-4.9
	PLP	-6.1
		-5.8
		-5.7
CL3	Lysine	-4.3
CL4	Lysine	-5.7
CL5	Lysine	-4.6
		-4.7
	PLP	-5.5
		-5.5
CL6	Lysine	-4.7
		-4.4
	PLP	-5.4

Structural analysis and in vitro **assay of the effective mutant**.

For the structural comparison of CadA and LdcC, AlphaFold and ESMFold were employed, with ESMFold proving particularly suitable for predicting the structure of the chimeric mutant [30]. At alkaline pH, it is believed that the increased performance of the enzyme is primarily due to its ability to maintain its oligomeric state and remain insensitive to pH changes. Therefore, because the active sites for CadA activity were created by the dimerization of each enzyme monomer, dimerization fragments were the focus. Each region was assessed for its contribution to interactions in the dimeric complex (Fig. 5). By measuring the number of interacting residues (within 5 Å) and interaction energy (ddG) between the fragments of dimer, region 2 of CadA was predicted to be the most critical region for dimer formation.

Next, a simulation of substrate and cofactor binding was performed to explore other potential factors. The results revealed that LdcC and CL2 exhibited higher lysine-binding and PLP-binding energies than CadA and the other chimeric proteins (Table 1, p-value < 0.005). These findings suggest that, in addition to the oligomeric state, increased binding affinity of CL2 to this cofactor may have contributed to enhanced cadaverine production. Meanwhile in the case of CL4 showing significantly improved lysine-binding energy, the cadaverine production was lower than that of CL2, which seems likely due to impairment in catalytic conversion after binding.

Furthermore, the PLP-SD of CadA changed with the pH in its active and inactive forms. The PLP-SD region of CadA in its active form has a structure similar to that of LdcC [17]. Based on these factors, it is anticipated that fragments related to dimerization or those containing the pH-insensitive part of LdcC in the PLP-SD region, when combined with CadA, will generate a mutant that integrates the advantageous traits of both enzymes, exhibiting high catalytic activity and structural stability at high pH.

To assess the pH stability of CadA and CL2, lysate-based conversion assay performed under various pH conditions using strains expressing the wild-type CadA or the CL2 variants (Fig. 6). At acidic pH (5.0 and 6.0), both enzymes showed similar levels of activity. As the pH increased to 7.0 and 8.0, enzyme activities increased for both variants, but the increase was more pronounced for CL2, resulting in a greater activity difference between the two. At pH 9.0, although both enzymes showed reduced activity, CL2 retained 70.6% of its maximal activity (measured at pH 7.0), while CadA retained only 27.5%. These results demonstrate that CL2 maintains its enzymatic activity better than CadA under alkaline conditions, indicating improved pH stability.

To compare the activities of the three enzymes under varying concentrations of PLP and lysine, enzyme assay was performed. First, the enzymatic activity was measured in a cell lysate-based assay using buffers with various concentrations of PLP. Given that the intracellular PLP concentration is approximately 10 μM [21], the assay was conducted across a range of lower PLP concentrations. The background PLP concentration in the assay mixture was estimated to be approximately 3.71 nM, based on cellular parameters and lysate preparation conditions. The detailed calculation is provided in the Methods section. This background PLP may have partially contributed to basal activity at low PLP concentrations, but it was not sufficient to obscure the relative activity differences among enzymes. CL2 exhibited the highest activity at all PLP concentrations, and all three enzymes showed a partial decrease in activity as the PLP concentration was reduced (Fig. 7). Notably, although CadA retained only 47.9% of its maximum activity at low PLP concentrations, LdcC had a significantly higher retention ratio of 61.5%. This trend was also observed for CL2, which retained 64.6% of its maximal activity. We hypothesized that the improved activity retention of CL2 at low PLP concentrations was due to its enhanced PLP affinity, which appeared to result from the introduction of the PLP-binding region of LdcC.

Then, kinetics of three variants were characterized with varied amount of lysine using purified enzymes (Table 2). The mutant exhibits a slightly lower K_m, indicating a marginally higher affinity, but also a slightly lower k_{cat},

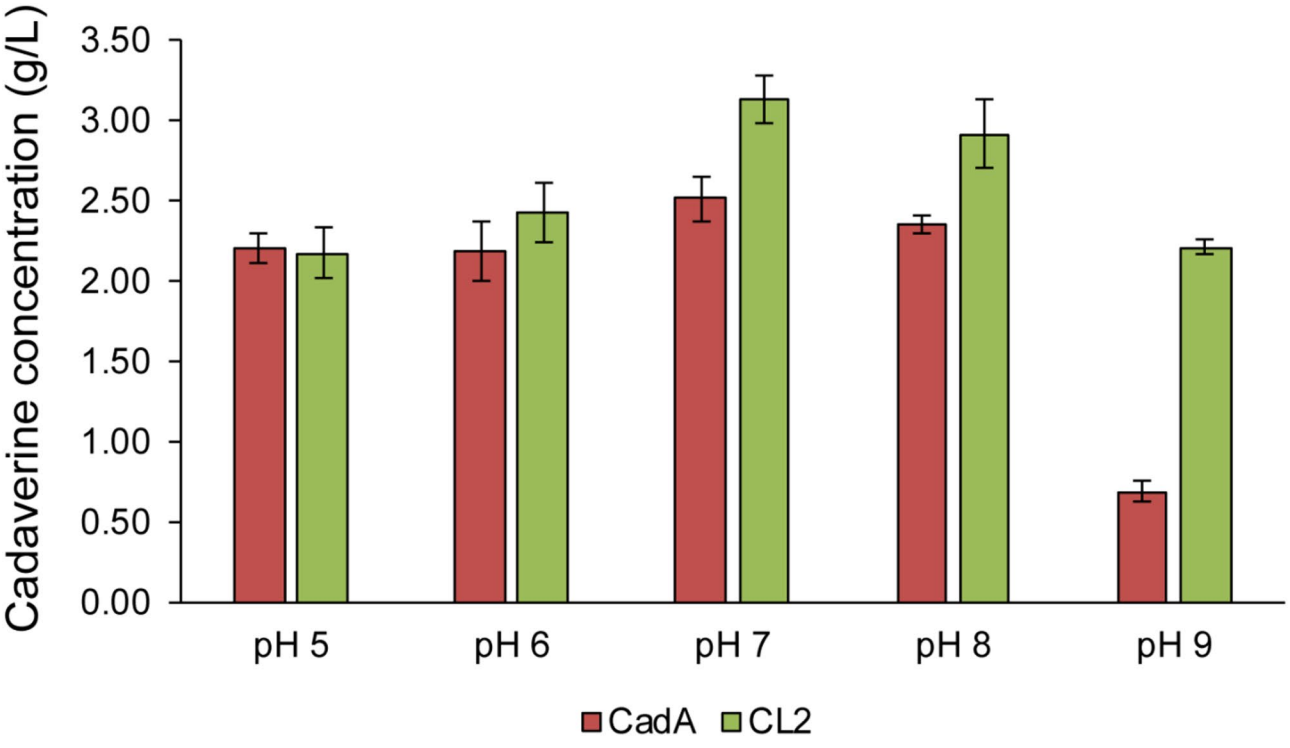

Fig. 6 Comparison of enzymatic activity between CadA and CL2 at different pH conditions
The enzymatic activity of wild-type CadA and CL2 was compared under different pH conditions (5, 6, 7, 8, and 9) by quantifying the cadaverine concentration converted from lysine. The error bars display the standards deviations of three biological replicates ($n = 3$)

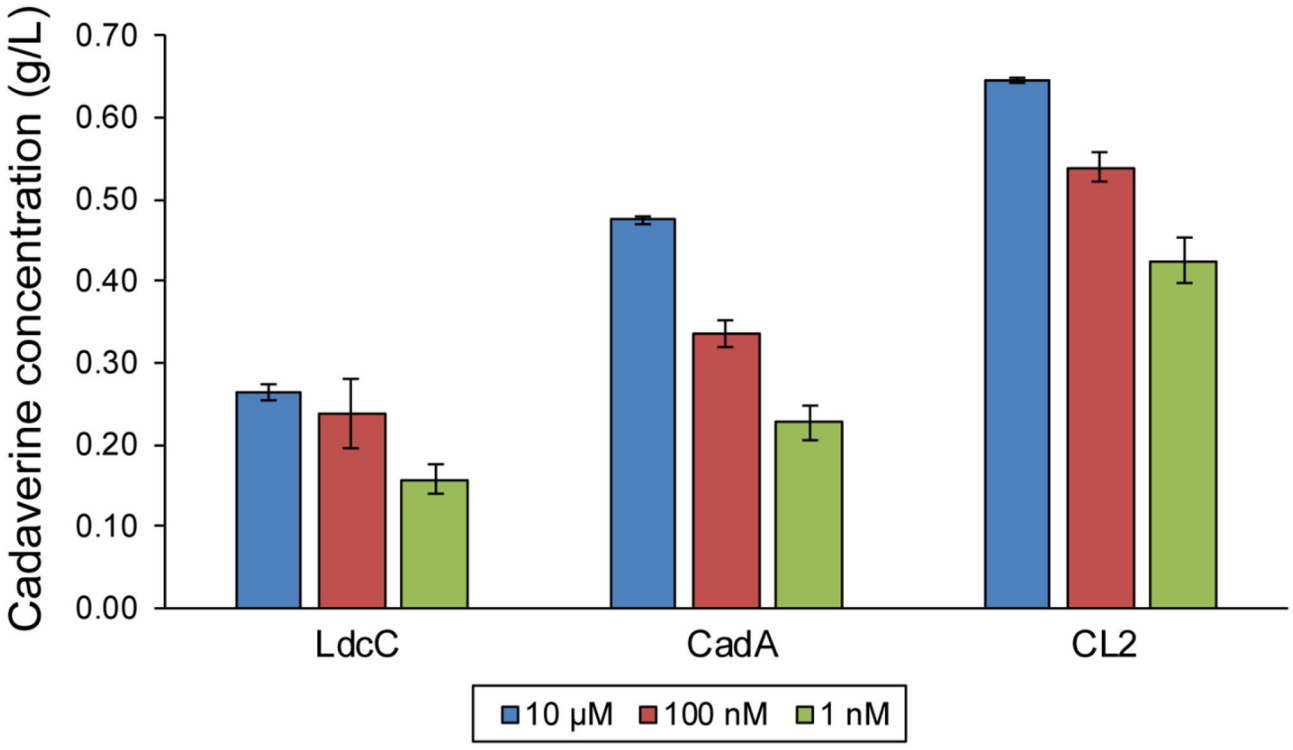

Fig. 7 Comparative analysis of the activity of three enzymes (LdcC, CadA, CL2) based on enzyme assay
The assays were conducted using buffers supplemented with varying concentrations of PLP (10 μM, 100 nM, and 1 nM). The error bars display the standard deviations of three biological replicates ($n = 3$)

Table 2 Kinetic parameters of lysine decarboxylases

Enzyme	K_m (mM)	Relative k_{cat}	Relative k_{cat}/K_m
LdcC	18.46 ± 0.89	1.00 ± 0.01	1.00 ± 0.04
CadA	29.23 ± 9.56	2.51 ± 0.81	1.58 ± 0.01
CL2	22.18 ± 5.73	1.81 ± 0.41	1.51 ± 0.04

resulting in a similar k_{cat}/K_m ratio. The improved lysine affinity may have contributed to the superior performance of CL2, particularly under lysine-limited conditions in vivo. In addition, its enhanced pH stability and more effective utilization of limited intracellular PLP are likely to further support the observed increase in cadaverine production during culture.

Discussion

The chimeric CadA engineered in this study demonstrated significantly enhanced cadaverine production due to improved pH stability and PLP-binding affinity. The structural modification, particularly focused on the oligomerization interface and PLP-binding subdomain, proved effective, resulting in a 1.96-fold increase in cadaverine production compared to wild-type CadA. Although previous studies have attempted to improve pH stability through random mutagenesis or rational design, targeting specific residues [12, 31, 32], our segmental swapping approach provides a more comprehensive solution by incorporating naturally evolved pH-stable regions from LdcC.

To achieve this, we applied a region-based segmental swapping strategy to generate chimeric enzymes between CadA and LdcC. The proteins were divided into six contiguous segments, each approximately 120 amino acids in length. This method was intentionally designed to differ from the classical "domain swapping" approach, which typically involves exchanging structurally independent and functionally annotated domains. Domain swapping has the advantage of preserving structural consistency and often preserving folding and activity but is inherently limited by prior assumptions about domain boundaries. In contrast, our segmental recombinant approach explores modularity at a finer resolution, allowing us to capture novel or distributed functional effects that do not correspond to the canonical domain architecture. With segmental swapping, we successfully engineered enzymes exhibiting high activity and enhanced pH tolerance. However, this technique must be applied with caution. In the absence of structural information, such segmental recombination can disrupt proper protein folding, often leading to non-functional variants. In our case, structural and sequence analyses indicated a high degree of similarity between CadA and LdcC, suggesting that overall structural integrity could be preserved even without precise domain-based swapping. Computational predictions

using AlphaFold and ESMFold further supported that the global folding of the protein could be preserved. In the future, further refinement through additional segmental swaps will help dissect the functional contributions of individual regions and enhance our understanding of structure–function relationships in these enzymes.

The active site of lysine decarboxylase is formed through dimerization of its monomers. Region 2 of CadA, which plays a crucial role in this dimerization, was replaced with the corresponding part of LdcC, known for its lower sensitivity to high pH. This substitution resulted in the CL2 mutant, which demonstrated enhanced stability of its decameric structure at elevated pH. This improvement suggests that the oligomerization interface is critical for maintaining both enzyme stability and catalytic activity [17]. *E. coli* harbors two lysine decarboxylases with distinct characteristics: LdcC, which is constitutively expressed and functions over a broad pH range but exhibits low catalytic efficiency, and CadA, which is induced and active only under acidic conditions but possesses high catalytic efficiency. From an evolutionary perspective, CadA has likely evolved to exhibit high activity under acidic conditions to maintain pH homeostasis, while rapidly losing function at other pH levels to prevent unnecessary lysine consumption. To integrate the high catalytic efficiency of CadA with the structural stability of LdcC, we employed segmental swapping to engineer CL2, enabling it to retain high activity even at neutral or higher pH, thereby enhancing intracellular cadaverine production.

The improved PLP binding affinity of CL2 represents another significant advancement in this regard. The retention of 61.1% activity at low PLP concentrations, compared to 44.1% for wild-type CadA, indicated that the engineered enzyme could maintain higher stability when cofactor availability might be limited. These data are supported by the docking simulation between the enzyme and PLP listed in Table 1. CL2 is expected to retain cadaverine production even at low PLP concentrations, as it has acquired the strong PLP-binding energy characteristic of LdcC. This characteristic could potentially reduce the process costs associated with PLP supplementation, thus addressing a key economic constraint in large-scale cadaverine production [12, 21]. Our structural analysis revealed that the PLP-SD region of active CadA shares conformational similarities with LdcC, providing a molecular basis for successful segmental swapping. While the current study focused on enzyme engineering, further improvements in cadaverine production could be achieved by integrating metabolic engineering strategies, particularly through the deletion of *speE*, *speG*, and *patA*, combined with the optimization of lysine biosynthesis [9, 29].

Conclusion

In the current study, this not only provides an improved biocatalyst for cadaverine production, but also demonstrates the effectiveness of structure-aware segmental swapping as a protein engineering strategy. The successful integration of the advantageous properties of homologous enzymes suggests that this approach could be particularly valuable for engineering industrial biocatalysts where multiple performance parameters need to be simultaneously optimized.

Abbreviations

PLP Pyridoxal 5-phosphate;
SD Subdomain

Supplementary Information

The online version contains supplementary material available at https://doi.org/10.1186/s12934-025-02739-4.

Supplementary Material 1

Author contributions

S.K. and D.Y. are contributed equally to this work. S.K., D.Y., H.G.L., M.H.N., J.-S.Y., and G.Y.J. conceived the project, conducted data analysis and interpretation, and wrote the manuscript. S.K. and D.Y. designed and conducted the experiments. M.H.N., J.-S.Y., and G.Y.J. supervised the project. All the authors read and approved the final manuscript.

Funding

This research was supported by the National Research Foundation of Korea (NRF) grants (RS-2024-00400033 and RS-2024-00453085) funded by the Ministry of Science and ICT. We also acknowledge RYC2020-028880-I funded by MCIN/AEI/10.13039/501100011033 and by "ESF Investing in your future".

Data availability

No datasets were generated or analysed during the current study.

Declarations

Competing interest

The authors declare that they have no known competing financial interests or personal relationships that could have appeared to influence the work reported in this paper.

Received: 7 January 2025 / Accepted: 5 May 2025
Published online: 22 May 2025

References

1. Ma W, Chen K, Li Y, Hao N, Wang X, Ouyang P. Advances in cadaverine bacterial production and its applications. Engineering. 2017;3:308–17.
2. Tomar PC, Lakra N, Mishra SN. Cadaverine: a lysine catabolite involved in plant growth and development. Plant Signal Behav. 2013;8. https://doi.org/10.4161/psb.25850.
3. Huang C-Y, Ting W-W, Chen Y-C, Wu P-Y, Dong C-D, Huang S-F, et al. Facilitating the enzymatic conversion of Lysineto cadaverine in engineered *Escherichia coli* with metabolic regulation by genes deletion. Biochem Eng J. 2020;156:107514.
4. Huang Y, Ji X, Ma Z, Łężyk M, Xue Y, Zhao H. Green chemical and biological synthesis of cadaverine: recent development and challenges. RSC Adv. 2021;11:23922–42.
5. Kovács T, Mikó E, Vida A, Sebő É, Toth J, Csonka T, et al. Cadaverine, a metabolite of the microbiome, reduces breast cancer aggressiveness through trace amino acid receptors. Sci Rep. 2019;9:1300.

6. Kim J-H, Seo H-M, Sathiyanarayanan G, Bhatia SK, Song H-S, Kim J, et al. Development of a continuous l-lysine bioconversion system for cadaverine production. J Ind Eng Chem. 2017;46:44–8.
7. Kind S, Neubauer S, Becker J, Yamamoto M, Völkert M, von Abendroth G, et al. From zero to hero - production of bio-based nylon from renewable resources using engineered *Corynebacterium glutamicum*. Metab Eng. 2014;25:113–23.
8. Rui J, You S, Zheng Y, Wang C, Gao Y, Zhang W, et al. High-efficiency and low-cost production of cadaverine from a permeabilized-cell bioconversion by a Lysine-induced engineered *Escherichia coli*. Bioresour Technol. 2020;302:122844.
9. Kwak DH, Lim HG, Yang J, Seo SW, Jung GY. Synthetic redesign of *Escherichia coli* for cadaverine production from galactose. Biotechnol Biofuels. 2017;10:20.
10. Qian Z-G, Xia X-X, Lee SY. Metabolic engineering of *Escherichia coli* for the production of cadaverine: a five carbon Diamine. Biotechnol Bioeng. 2011;108:93–103.
11. Wang X, Guo X, Wang J, Li H, He F, Xu S, et al. Ameliorating end-product Inhibition to improve cadaverine production in engineered *Escherichia coli* and its application in the synthesis of bio-based diisocyanates. Synth Syst Biotechnol. 2021;6:243–53.
12. Sagong H-Y, Kim K-J. Lysine decarboxylase with an enhanced affinity for pyridoxal 5-Phosphate by disulfide Bond-Mediated Spatial reconstitution. PLoS ONE. 2017;12:e0170163.
13. Kim HJ, Kim YH, Shin J-H, Bhatia SK, Sathiyanarayanan G, Seo H-M, et al. Optimization of direct lysine decarboxylase biotransformation for cadaverine production with Whole-Cell biocatalysts at high lysine concentration. J Microbiol Biotechnol. 2015;25:1108–13.
14. Park SH, Soetyono F, Kim HK. Cadaverine production by using Cross-Linked enzyme aggregate of *Escherichia coli* lysine decarboxylase. J Microbiol Biotechnol. 2017;27:289–96.
15. Kikuchi Y, Kojima H, Tanaka T, Takatsuka Y, Kamio Y. Characterization of a second lysine decarboxylase isolated from *Escherichia coli*. J Bacteriol. 1997;179:4486–92.
16. Lemonnier M, Lane D. Expression of the second lysine decarboxylase gene of *Escherichia coli*. Microbiol (Reading Engl). 1998;144(Pt 3):751–60.
17. Kandiah E, Carriel D, Perard J, Malet H, Bacia M, Liu K, et al. Structural insights into the *Escherichia coli* lysine decarboxylases and molecular determinants of interaction with the AAA + ATPase RavA. Sci Rep. 2016;6:24601.
18. Shah P, Swiatlo E. A multifaceted role for polyamines in bacterial pathogens. Mol Microbiol. 2008;68:4–16.
19. Xi Y, Ye L, Yu H. Enhanced thermal and alkaline stability of L-lysine decarboxylase CadA by combining directed evolution and computation-guided virtual screening. Bioresour Bioprocess. 2022;9:24.
20. Yamada H, Yamaguchi M, Shimizu K, Murayama SY, Mitarai S, Sasakawa C, et al. Structome analysis of *Escherichia coli* cells by serial ultrathin sectioning reveals the precise cell profiles and the ribosome density. Microscopy (Oxf). 2017;66:283–94.
21. Ma W, Cao W, Zhang B, Chen K, Liu Q, Li Y, et al. Engineering a pyridoxal 5′-phosphate supply for cadaverine production by using *Escherichia coli* whole-cell biocatalysis. Sci Rep. 2015;5:15630.
22. Beninati S, Martinet N, Folk JE. High-performance liquid chromatographic method for the determination of ε-(γ-glutamyl)lysine and mono- and bis-γ-glutamyl derivatives of Putrescine and spermidine. J Chromatogr A. 1988;443:329–35.
23. Yang J, Seo SW, Jang S, Shin S-I, Lim CH, Roh T-Y, et al. Synthetic RNA devices to expedite the evolution of metabolite-producing microbes. Nat Commun. 2013;4:1413.
24. Kanjee U, Gutsche I, Alexopoulos E, Zhao B, El Bakkouri M, Thibault G, et al. Linkage between the bacterial acid stress and stringent responses: the structure of the inducible lysine decarboxylase. EMBO J. 2011;30:931–44.
25. Pettersen EF, Goddard TD, Huang CC, Couch GS, Greenblatt DM, Meng EC, et al. UCSF Chimera—a visualization system for exploratory research and analysis. J Comput Chem. 2004;25:1605–12.
26. Lin Z, Akin H, Rao R, Hie B, Zhu Z, Lu W et al. Evolutionary-scale prediction of atomic-level protein structure with a Language model. Science. 2023.
27. Yan Y, Tao H, He J, Huang S-Y. The HDOCK server for integrated protein-protein Docking. Nat Protoc. 2020;15:1829–52.
28. Kou F, Zhao J, Liu J, Shen J, Ye Q, Zheng P et al. Characterization of a new lysine decarboxylase from *Aliivibrio salmonicida* for cadaverine production at alkaline pH. J Mol Catal B: Enzymatic. 2016.
29. Qian Z-G, Xia X-X, Lee SY. Metabolic engineering of *Escherichia coli* for the production of Putrescine: a four carbon Diamine. Biotechnol Bioeng. 2009;104:651–62.
30. Fang Y, Jiang Y, Wei L, Ma Q, Ren Z, Yuan Q et al. DeepProSite: structure-aware protein binding site prediction using ESMFold and pretrained Language model. Bioinformatics. 2023;39.
31. Gao S, Zhang A, Ma D, Zhang K, Wang J, Wang X, et al. Enhancing pH stability of lysine decarboxylase via rational engineering and its application in cadaverine industrial production. Biochem Eng J. 2022;186:108548.
32. Kou F, Zhao J, Liu J, Sun C, Guo Y, Tan Z, et al. Enhancement of the thermal and alkaline pH stability of *Escherichia coli* lysine decarboxylase for efficient cadaverine production. Biotechnol Lett. 2018;40:719–27.

Publisher's note